RESEARCH ARTICLE

INTERNATIONAL MICROBIOLOGY (2006) 9:289-295
www.im.microbios.org

INTERNATIONAL MICROBIOLOGY

Jacek Wierzchos[1]
Mercedes Berlanga[2]*
Carmen Ascaso[3]
Ricardo Guerrero[4]

[1]Electronic Microscopy Service, University of Lleida, Spain
[2]Department of Microbiology and Parasitology, Faculty of Pharmacy, University of Barcelona, Spain
[3]Environmental Science Research Center, CSIC, Madrid, Spain
[4]Department of Microbiology, Faculty of Biology, University of Barcelona, Spain

Micromorphological characterization and lithification of microbial mats from the Ebro Delta (Spain)

Summary. The structural organization of microbial mats from the Ebro Delta (Spain) and their accretion and partial lithification processes were explored using scanning electron microscopy in back-scattered electron mode and low-temperature scanning electron microscopy. Two differentiated zones were distinguished in a transverse section of a fragment taken from the mat at a depth of 2.5 mm. The first consisted of an upper layer in which the dominant microorganisms, *Microcoleus* spp., actively grew in an embedded slack matrix of exopolysaccharides. *Microcoleus* filaments were oriented parallel to the surface and to each other, with filaments below arranged perpendicularly to one another but without crossing. Most of the minerals present were allochthonous grains of calcium phosphate biocorroded by cyanobacteria. The second zone was below a depth of 1 mm and made up of accretion layers with large deposits of calcium carbonate and smaller amounts of calcium phosphate of biological origin. The predominance of a particular type of mineral precipitation with a characteristic external shape and/or texture within a zone, e.g., sponge-like deposits of calcium phosphate, appears to depend on the taxa of the prevailing microorganisms. [**Int Microbiol** 2006; 9(4):289-295]

Key words: *Microcoleus chthonoplastes* · microbial mats · accretion · lithification · biofilms

Received 15 June 2006
Accepted 10 September 2006

*Corresponding author:
M. Berlanga
Dpt. of Microbiology and Parasitology
Faculty of Pharmacy
University of Barcelona
Av. Joan XXIII, s/n
08028 Barcelona, Spain
Tel. +34-934024497. Fax +34-934024498
E-mail: mberlanga@ub.edu

Introduction

Microbial mats are multilayered biofilms. Their lamination results from a light gradient along the vertical axis and from physicochemical microgradients generated by the metabolism of the component prokaryotic populations. These layers, which are apparent even macroscopically, show active growth and span thicknesses ranging from a few millimeters to several centimeters. The microbial diversity and community structure of microbial mats have been examined by a variety of microscopy techniques, such as light microscopy, scanning and/or transmission electron microscopy (SEM, TEM) [16,25], and confocal laser scanning microscopy (CLSM) [7]. The ordered spatial arrangement of microorganisms reflects their enormously complex functional interactions [8,9,14]. Microbial mats dominated Archaean landscapes. Their presence in the fossil record is documented by the laminated sedimentary rock structures called stromatolites. Stromatolites are organosedimetary structures produced by the trapping, binding, and precipitation of minerals as a result of the growth and metabolic activity of microorganisms [2]. The persistence and abundance of stromatolites throughout geological history attest to the evolutionary suc-

cess of microbial mat ecosystems. Indeed, stromatolites have been found in rocks ca. 3,500 million year old [1,22].

Depending on the prevailing environmental conditions and the activities of indigenous microbial populations, individual cells can facilitate the crystal nucleation of different minerals [21]. Mineral precipitation may be promoted by: (i) changes in microenvironmental chemical conditions and hence saturation state as a result of microbial metabolic processes, (ii) nucleation on the surfaces of microorganisms (e.g., the cell envelope is very important for calcification) or on microbial products. Visscher et al. [28] correlated sulfate-reduction activity with high zones of $CaCO_3$ precipitation in modern marine stromatolites, although the biogeochemical processes of accretion and mineralization (lithification) of mat systems are poorly understood. Modern microbial mats are usually viewed as analogues of ancient stromatolites, but a major difference between extent mats and ancient stromatolite-forming mats is that the latter have lithified laminae that form domal or columnar structures. Why ancient stromatolites and "modern living stromatolites," such as those from Shark Bay in Western Australia and the Exuma Sound in Bahamas, form lithified laminae, whereas other microbial mats do not, is still unresolved.

In situ analysis using SEM in back-scattered electron detection mode (BSE) may offer a better perspective on the building processes involved in the formation of microbial structures, such as lithified laminae. The resolution of SEM-BSE is similar to that of SEM with secondary electrons and the ultrastructural information is comparable to that obtained with TEM. Moreover, SEM-BSE can be combined with energy dispersive X-ray spectroscopy (EDS) microanalysis to provide high resolution of the mineral features of specific microhabitats surrounding microorganisms. The purpose of the present study was to use these techniques to provide detailed information on the community structure of microbial mats and microbe-mineral interactions.

Materials and methods

Sampling site and sample collection. The zone selected for sampling was located in La Banya spit, in the southern peninsula of the Ebro Delta (Spain). This site, which harbored well-developed microbial mats, was designated point G (40º 35′ 28″ N, 0º 39′ 39″ E) [13]. Samples were collected in the spring at noon from different locations of the surrounding ponds and at a depth of about 5 cm. Squares (3 × 3 cm) were cut from cohesive layers and placed on a plastic tray. In this way, several cores could be removed using a metal corer with an inner diameter of 5 mm. These mat cores were placed in porous plastic cylinders of similar diameter and then processed for SEM-BSE and EDS microanalysis.

Scanning electron microscopy with back-scattered electron imaging combined with a microanalytical system. Mat cores were processed for in situ visualization by SEM-BSE. Details of this preparative procedure can be found in Wierzchos and Ascaso [29]. Briefly, the sample was fixed in glutaraldehyde and then stained with osmium tetroxide and/or uranyl acetate, which yielded finely polished blocks containing the resin-embedded samples. The BSE signal is strongly dependent on the mean atomic number of the target. Thus, the SEM-BSE procedure enables samples with different inorganic features to be visualized and ultrastructural elements of microorganisms to be identified by staining with heavy metals. Transverse sections of the finely polished blocks containing microbial mat samples were examined using a DSM 942A Zeiss instrument equipped with a BSE solid-state detector. The EDS system (Link ISIS Oxford) is coupled to the SEM-BSE instrument, which permits chemical characterization of mineral features (such as the qualitative and quantitative determination of elements), and yields images of the spatial distribution of the component elements. The operating conditions for the microscopy and microanalytical procedures were provided in Wierzchos et al. [30].

Low-temperature scanning electron microscopy. This technique was carried out as described by De los Ríos et al. [6,7]. Briefly, samples were kept in the fully hydrated state and then fixed mechanically onto the specimen holder of an Oxford CT1500 cryotransfer system. This instrument plunge-freezes the samples in subcooled liquid nitrogen and then transfers them to the preparation unit, where they are fractured. The samples were coated by gold sputtering and then examined on the cold stage of a DSM 960 Zeiss SEM microscope.

Results

In situ morphological and structural characteristics of the Ebro Delta mats. In situ SEM-BSE observations provided morphological and, perhaps more importantly, ultrastructural information on the benthic microorganisms. The method allows continuous visualization from low to high magnification (Fig. 1A–D). For example, the SEM-BSE micrograph in Fig. 1A shows a 0.6-mm-thick cross-section of a microbial mat, and details of this microbial community can be observed at higher magnification (Fig. 1B–D). The cross-section is dominated by the filamentous, sheathed cyanobacterium *Microcoleus chthonoplastes*. The abundance of these cyanobacteria was estimated by Garcia-Pichel et al. [11] as the percentage of the area occupied by *Microcoleus* spp. Colonization by *Microcoleus* spp. diminished with depth: approximately 40% in the first 0.15 mm, 31% from 0.15 to 0.30 mm, and less than 10% in deeper layers, as previously observed [16]. The lamination profile of the whole sample consisted of an upper layer (up to 0.3 mm) of loose matrix underlain by a more or less compact layer (between 0.3 and 0.4 mm in depth) containing an exopolysaccharide network, in which sheathed cyanobacteria were also observed, and finally, another dense layer in which no filamentous cyanobacteria were visible (usually below 0.4–0.5 mm). In the upper part of the cross-section, *Microcoleus* filaments ran parallel to the surface and to each other, whereas the filaments in the other layers were often oriented perpendicularly to each other but without crossing. Thus, filamentous *Microcoleus chthonoplastes* was the dominant biota

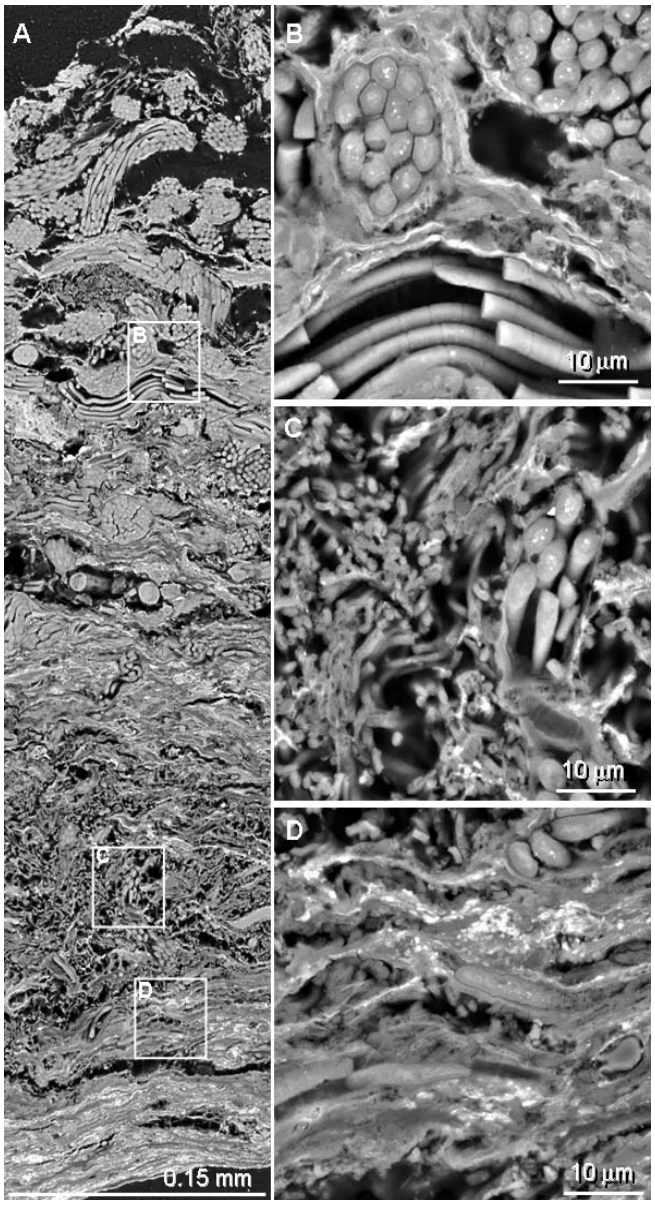

Fig. 1. SEM-BSE micrographs of a microbial mat sample from the Ebro Delta. (**A**) Cross-section of a 0.6-mm thick microbial mat [IM 5(4) p184]. (**B**–**D**) Detailed views of the areas outlined in (A) of microbial communities, showing the presence of the cyanobacterium *Microcoleus chthonoplastes*.

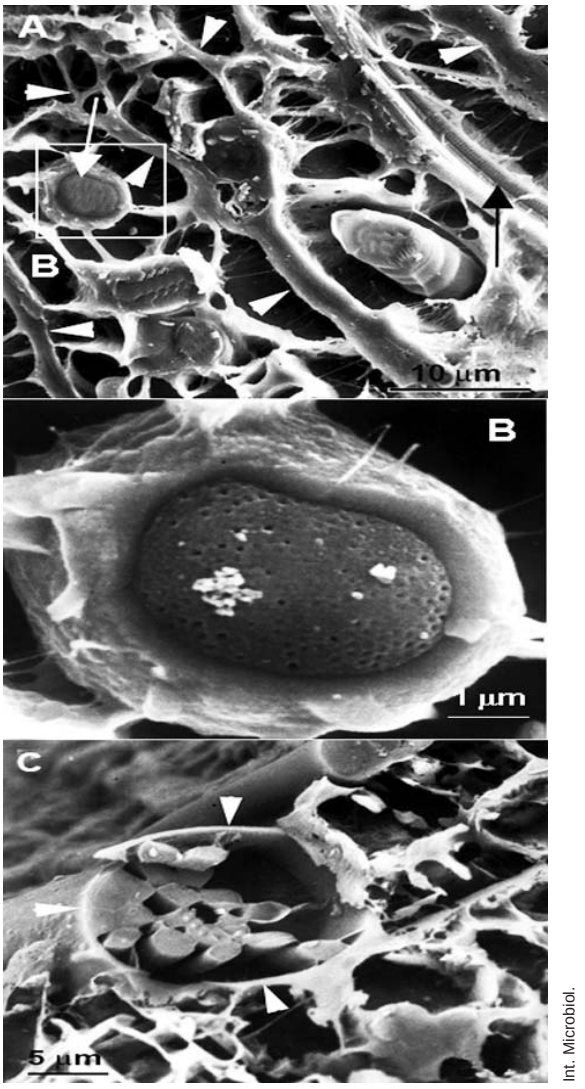

Fig. 2. LT-SEM images showing filamentous cyanobacteria and exopolysaccharides in a microbial mat sample from the Ebro Delta. (**A**) Transversely sectioned filamentous cyanobacteria are surrounded by extracellular polysaccharide substances (arrowheads). The white arrow points to the cyanobacterial cell membrane and the black arrow points to the diatom frustule. (**B**) Magnification of a cyanobacterium from (A). (**C**) Transversely sectioned *Microcoleus chthonoplastes* cyanobacteria enclosed in an exopolysaccharide sheath (arrowheads).

of the upper layer of these Ebro Delta mats and seemed to determine their basic structure. A similar layered structure was described by Kühl and Fenchel [18]. The mechanism behind the spatial ordering of cyanobacterial filaments is unclear but may involve photosensory motile behavior or geometric constraints related to filament reproduction [10,18].

LT-SEM provides topographical images of randomly fractured planes of deep-frozen samples. The surface of such fractures in the microbial mat samples can be seen in Fig. 2. Several cyanobacterial cells appear circular in cross-section (Fig. 2A), and ultrastructural elements, such as the cell membrane, can be observed in cryofixed cells (white arrow in Fig. 2A); Fig. 2A also shows a diatom frustule (black arrow). Since cryofixed specimens do not undergo chemical fixation, not only the cells but also the extracellular polysaccharide substances (arrowheads in Fig. 2A) surrounding them can be seen. Figure 2B is an inset of 2A. Figure 2C shows a transverse section of filamentous cyanobacterial streams enclosed in sheaths of extracellular polysaccharides (arrowheads). LT-SEM can also provide information about the hydration state

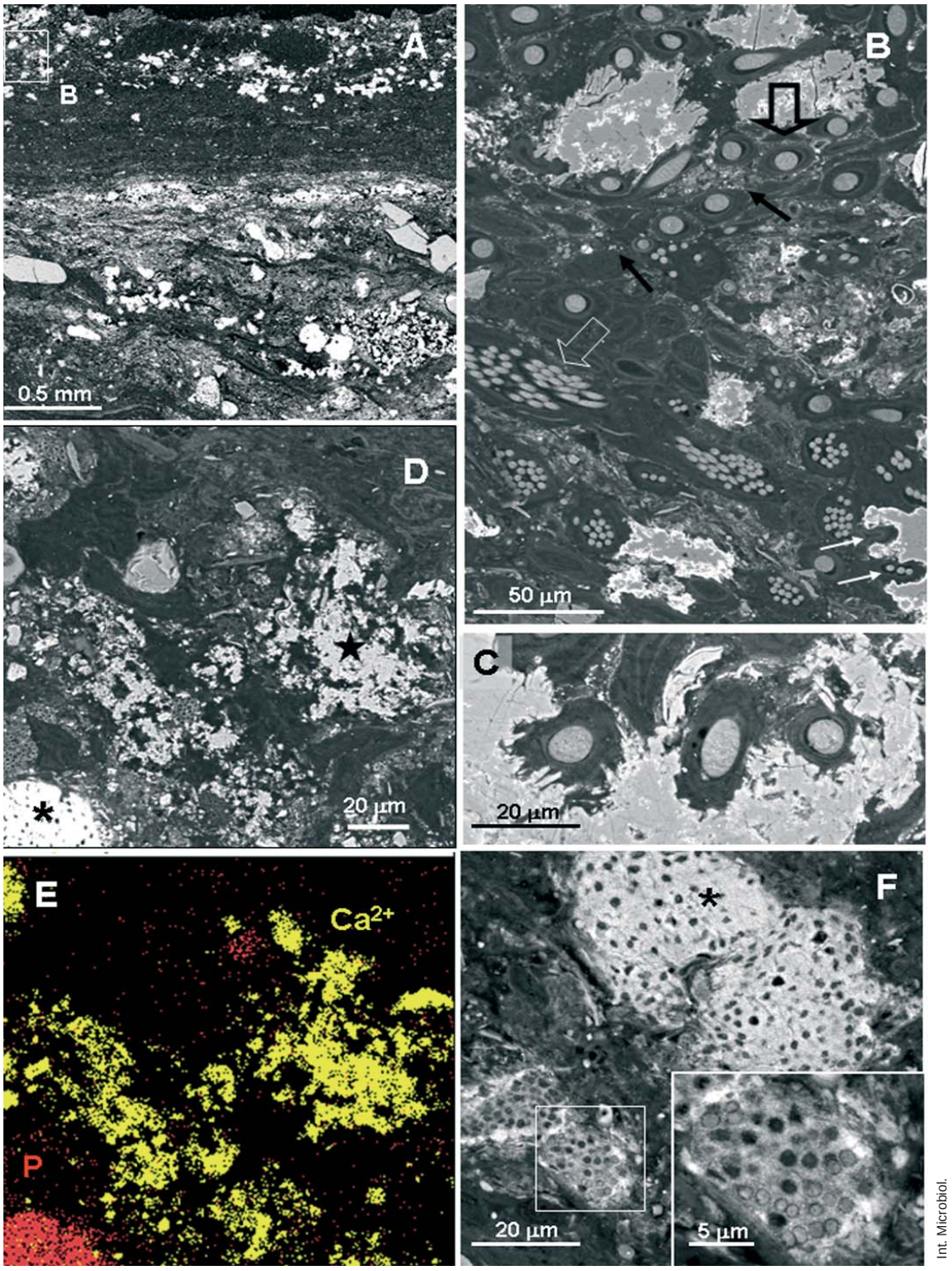

Fig. 3. SEM-BSE and EDS images of allochthonous and bioaccumulated inorganic deposits in a microbial mat sample from the Ebro Delta. (**A**) SEM-BSE low-magnification image of a cross section taken at a depth of 0–2.6 mm. (**B**) SEM-BSE image of a cross-section taken at a depth of 0.25 mm, showing *Microcoleus* spp. (open white arrow) and *Lyngbya* spp. (black open arrow) cyanobacteria. White arrows indicate the biocorosive action (euendolithic) of *Microcoleus* spp. on a calcium phosphate grain and black arrows indicate aluminosilicate clay coatings around cyanobacteria. (**C**) Detailed view of the euendolithic action of *Lyngbya* spp. on a $Ca_3(PO_4)_2$ grain. (**D**) SEM-BSE image of a lithified layer (2 mm depth) of a microbial mat, showing calcium carbonate (star) and calcium phosphate biodeposits (asterisk). (**E**) EDS element distribution maps of phosphorus (indicating a calcium phosphate phase) and calcium (indicating a calcium carbonate phase) corresponding to D. (**F**) Detailed SEM-BSE view of calcium phosphate sponge-like deposits formed around the bacterial cells, an enlargement of which is provided in the square. Asterisk indicates an older deposit with no live bacterial cells.

of the cell and/or the presence of intra- or intercellular water (ice) [6,7]; however, water was not observed in the biological components of the microbial mats studied here.

Lithification of microbial mats. Transverse sections corresponding to different depths of the microbial mats revealed different stages of accretion or lithification (Fig. 3A). The low-magnification SEM-BSE image of Fig. 3A shows stratification of the mineral components of the top 2.6 mm of the mat. EDS elemental distribution maps (Fig. 3B, C) indicated that the upper layer (up to a depth ca. 1 mm) contained randomly distributed calcium phosphate grains while deeper layers (from 1 to 2.5 mm) were mostly occupied by calcium carbonate deposits that had formed in situ. A closer view of the upper layer in Fig. 3A is shown in the top left-hand corner of Fig. 3B. This image shows the presence of filamentous, sheathed cyanobacteria of the species *Microcoleus* and *Lyngbya*. Streams of *Microcoleus* spp. and filaments of *Lyngbya* spp. appear to be coated with fine aluminosilicate clay particles, which were detected by EDS microanalysis. The mineral phase in this upper layer was mostly composed of allochthonous calcium phosphate grains about 50-80 μm in diameter. The source of these grains may have been aeolian contamination and/or mineral suspensions in the flowing water. Filamentous cyanobacteria produce a tough network in which sediment particles such as these may be entrapped. Alternatively, it has been observed that cyanobacterial species actively interact with calcium phosphate grains, leading to dissolution of the grain surface and biomobilization of calcium and phosphate ions. This euendolithic action [12] of *Microcoleus* spp. and *Lyngbya* spp. can be seen in Fig. 3B and 3C, respectively.

At an approximate depth of 0.5-1 mm, there was a thin mineral layer containing a few live cells, such as *Microcoleus chthonoplastes* and *Lyngbya* spp., interspersed with dead, sheathed cells that are empty or collapsed (Fig. 1A, 3A). The layer beneath a depth of 1 mm in this microbial mat was extensively mineralized (Fig. 3A,D). Microbial cells promote sediment accretion by selectively incorporating coarse allochthonous sediment grains, such as quartz and/or feldspars [17]. The dominant bioaccumulated, in-situ-formed mineral in this layer was fine crystalline calcium carbonate, which had subsequently aggregated (star in Fig. 3D). Figure 3E provides the EDS calcium spatial distribution map for the SEM-BSE image shown in Fig. 3D, in which these large calcium carbonate deposits can be seen in the spaces between dead cells. In the same layer, newly formed deposits of calcium phosphate were also observed (asterisks in Figs. 3D, 3E and 3F). The EDS distribution map for phosphorus and EDS point analysis (data not shown) distinctly indicated that the in situ-formed deposits were composed of $Ca_3(PO_4)_2$. Bioaccumulation of calcium phosphate is known to occur around bacterial cells. In the early stages of deposit formation, many live bacterial cells are present within the fine crystalline calcium phosphate, as is the case in the example shown in Fig. 3F. When the bacterial cells dye, the calcium phosphate deposits become much more compact, with small voids that render them with a sponge-like appearance (asterisks in Fig. 3F).

Discussion

To understand the role of microbial mats in precipitation and dissolution, it is important to determine both the abundance and the metabolic activity of the "guilds" (functional groups) [15]. The layered microbial mats of the Ebro Delta are primarily composed of communities of oxygenic photoautotrophs: diatoms, cyanobacteria (*Microcoleus* and *Lyngbya*; Figs. 1, 2), anoxygenic photoautotrophs (the purple sulfur bacteria *Chromatium* and *Thiocapsa,* and the green sulfur bacteria *Chlorobium*), chemoautotrophs (colorless sulfur bacteria, such as *Thiobacillus* and *Beggiatoa*), heterotrophs (several metabolic kinds of bacteria, e.g., the characteristic morphophysiological group of the spirochetes), and sulfate-reducing bacteria [20]. Moreover, molecular techniques have facilitated the detection and identification of many phylogenetic groups not previously observed [19]. Both the microbial activity and the specific taxa that characterize the mat determine the precipitation of substances (e.g., exopolymers) and the saturation index, which depends on the pH and the presence of ions (e.g., Ca^{2+} and CO_3^{2-}) in the environment.

In the flat laminated microbial mats examined in the present study, partial lithification did not occur at the surface but rather at some depth and after the cyanobacteria had died (Fig. 3). It has been observed that photosynthesis and aerobic respiration in the upper layers of mats do not result in net lithification [27]. In the upper layer of the mats studied here, actively growing microorganisms were embedded in a loose matrix of organic polymers (Fig. 1). Underlying this top layer was another layer consisting of exopolysaccharide sheaths with different extents of accretion indicative of calcium carbonate precipitation (Fig. 3) [23]. Mineralization (e.g., calcification) of dead cyanobacterial material is probably the result of carbonate precipitation by heterotrophic bacteria living on and from the organic material of the sheath [4,5]. Here, calcium carbonate biodeposits were observed in close proximity to decayed cyanobacterial filaments. Indeed, in most environments, carbonate production by heterotrophic bacteria is potentially much higher than that resulting from autotrophic or chemical sedimentation processes [17,23].

Regardless of whether cyanobacteria are directly involved in carbonate precipitation or not, the primary role of *Microcoleus* spp. in accretion and lithification, such as observed in the mat from the Ebro Delta, could be to produce exopolysaccharides, which trap and bind any unconsolidated sediments. This, in turn, might facilitate crystal nucleation, such that after the death of the sheathed cyanobacteria, heterotrophic bacteria would decompose the sheaths, which would then undergo mineralization. A similar process was suggested by Stolz et al. [26] for stromatolites from Highborne Cay, Bahamas, in which the dominant microorganism is *Schizothrix gebeleinii*. In addition, the type of mineral precipitation that predominates in a particular zone appears to depend on the inhabiting microorganisms and their preferences for particular chemical compounds. Since the structure of microbial mats is known to be determined by the dominant microorganisms [9], mats dominated by *Microcoleus* spp., even in different geographical areas, are likely to undergo similar accretion and lithification processes.

The bioaccumulation of calcium phosphate (apatite) observed in the deep mat layer and the mechanisms of precipitation of this mineral seemed to be closely related to the biological activity of the resident bacteria. It has been suggested that sulfur bacteria (e.g., *Beggiatoa*, *Thioploca*) should drive phosphogenesis and, under anoxic conditions, release enough phosphor to account for the precipitation of apatite or hydroxyapatite ($Ca_5OH[PO_4]_3$) [24]. In our samples, the sponge-like texture observed may have been produced by a combination of dissolution processes and the precipitation of apatite [3].

The microscopy and microanalytical methods used to examine microbial mats from the Ebro Delta provided in situ information spanning a resolution range from the single cell to the entire ecosystem. Through this unique approach, we were able to identify the taxa of microorganisms in their natural microenvironment, which is a basic requirement for characterizing microbial interactions with the mineral phase and/or lithification processes. The simultaneously provided microanalytical data contribute to a much more detailed understanding of mineral bioaccumulation processes and the role of microorganisms in them. Further insight into lithification in microbial mats could help bridge the gap between our knowledge of these modern ecosystems and their fossil homologues, stromatolites.

Acknowledgements. This work was supported by grants number BOS2003-02944 and CGL2005-04990/BOS (to RG), and REN2003-07366-C02-02 (to JW), from the Spanish Ministry of Education and Science.

References

1. Allwood AC, Walter MR, Kamber BS, Marshall CP, Burch IW (2006) Stromatolite reef from the early Archaean era of Australia. Nature 441:714-718
2. Awramik SM (2006) Respect for stromatolites. Nature 441:700-701
3. Blake RE, O'Neil JR, Garcia GA (1998) Effects of microbial activity on the d18O of dissolved inorganic phosphate and textural features of synthetic apatites. Am Mineral 83:1516-1531
4. Braissant O, Caillean G, Dupraz C, Verrecchia EP (2003) Bacterially induced mineralization of calcium carbonate in terrestrial environments: the role of exopolysaccharides and amino acids. J Sedim Res 73:485-490
5. Chafetz HS (1994) Bacterially induced precipitates of calcium carbonate and lithification in microbial mats. In: Krumbein WE, Paterson DM, Stal LJ (eds) Biostabilization of sediments. Universität Oldenburg (BIS)-Verlag, Oldenburg, pp 149-164
6. De los Ríos A, Ascaso C, Wierzchos J (1999) Study of lichens with different state of hydration by the combination of low temperature scanning electron and confocal laser scanning microscopies. Int Microbiol 2:251-257
7. De los Ríos A, Ascaso C, Wierzchos J, Fernández-Valiente E, Quesada A (2004) Microstructural characterization of cyanobacterial mats from the McMurdo ice shelf, Antarctica. Appl Environ Microbiol 70:569-580
8. Des Marais DJ (2003) Biogeochemistry of hypersaline microbial mats illustrates the dynamics of modern microbial ecosystems and the early evolution of the biosphere. Biol Bull 204:160-167
9. Dupraz C, Visscher PT (2005) Microbial lithification in marine stromatolites and hypersaline mats. Trends Microbiol 13:429-438
10. Fenchel T, Kühl M (2000) Artificial cyanobacterial mats: growth, structure, and vertical zonation patterns. Microb Ecol 40:85-93
11. García-Pichel F, Mechling MR, Castenholz W (1994) Diel migrations of microorganisms in a hypersaline microbial mat. Appl Environ Microbiol 60:1500-1511
12. Golubic SI, Friedmann EI, Schneider J (1981) The lithobiontic ecological niche, with spatial reference to microorganisms. J Sedim Petrol 51: 475-478
13. Guerrero R, Urmeneta J, Rampone G (1993) Distribution of types of microbial mats at the Ebro Delta, Spain. BioSystems 31:135-144
14. Guerrero R, Piqueras M, Berlanga M (2002) Microbial mats and the search for minimal ecosystems. Int Microbiol 5:177-188
15. Guerrero R, Berlanga M (2006) "Life's unity and flexibility": the ecological link. Int Microbiol 9:225-235
16. Jørgensen BB, Revsbech NP (1983) Photosyntesis and structure of benthic microbial mats: Microelectrode and SEM studies of four cyanobacterial communities. Limnol Oceanogr 28:1075-1093
17. Knorre H von, Krumbein WE (2000) Bacterial calcification. In: Riding RE, Awramik SM (eds) Microbial sediments. Springer-Verlag, Berlin, pp 25-31
18. Kühl M, Fenchel T (2000) Bio-optical characteristics and the vertical distribution of photosynthetic pigments and photosynthesis in an artificial cyanobacterial mat. Microb Ecol 40:94-103
19. Ley RE, Harris JK, Wilcox J, et al. (2006) Unexpected diversity and complexity of the Guerrero Negro hypersaline microbial mat. App Environ Microbiol 72:3685-3695
20. Martínez-Alonso M, Mir J, Caumette P, Gaju N, Guerrero R, Esteve I (2004) Distribution of phototrophic populations and primary production in a microbial mat from the Ebro Delta, Spain. Int Microbiol 7:19-25
21. Newman DK, Banfield JF (2002) Geomicrobiology: how molecular-scale interactions underpin biogeochemical systems. Science 296:1071-1077

22. Tice MM, Lowe DR (2004) Photosynthetic microbial mats in the 3,416 Myr-old ocean. Nature 431:549-552
23. Reid RP, Visscher PT, Decho AW, et al. (2000). The role of microbes in accretion, lamination and early lithification of modern marine stromatolites. Nature 406:989-992
24. Schulz HN, Schulz HD (2005) Large sulfur bacteria and the formation of phosphorite. Science 307:416-418
25. Stolz JF (1994) Light and electron microscopy in microbial mat research: An overview. In: Stal L, Caumette P (eds), Microbial mats: structure, development and environmental significance. NATO ASI Series. Series G: Ecological Sciences, vol. 35. Springer-Verlag, Berlin, pp 173-182
26. Stolz J, Feinstein FTN, Salsi J, Visscher PT, Reid RP (2001) TEM analysis of microbial sedimentation and lithification in modern marine stromatolites. Am Mineral 86: 826-833
27. Visscher PT, Reid RP, Bebout BM, Hoeft SE, Macintyre IG, Thompson JA Jr (1998) Formation of lithified micritic laminae in modern marine stromatolites (Bahamas): the role of sulfur cycling. Am Mineral 83: 1482-1493
28. Visscher PT, Reid RP, Bebout BM (2000) Microscale observations of sulfate reduction: correlation of microbial activity with lithified micritic laminae in modern marine stromatolites. Geology 28:919-922
29. Wierzchos J, Ascaso C (1994) Application of back-scattered electron imaging to the study of the lichen-rock interface. J Microsc 175:54-59
30. Wierzchos J, García Sancho L, Ascaso C (2005) Biomineralization of endolithic microbes in rocks from the McMurdo Dry Valleys of Antarctica: implications for microbial fossil formation and their detection. Environ Microbiol 7:566-575

Caracterización micromorfológica y litificación de los tapices microbianos del delta del Ebro (España)

Resumen. Se ha estudiado la organización estructural, acreción y litificación parcial de los tapices microbianos del delta del Ebro (España) mediante técnicas de microscopía electrónica de barrido en modo de electrones retrodispersados y de microscopía electrónica de barrido en bajas temperaturas. En una sección transversal de un fragmento de tapiz de 2,5 mm de profundidad, se observaron dos zonas diferenciadas. La primera era una capa superior en la que el microorganismo dominante es *Microcoleus* spp., en crecimiento activo y embebido en una matriz de exopolisacárido laxa. Los filamentos de *Microcoleus* se orientaban paralelamente a la superficie y eran paralelos entre ellos con los filamentos en la parte inferior, que se situaban de forma perpendicular pero sin llegar a cruzarse. La mayoría de los minerales presentes en esta zona eran granos de fosfato cálcico "biocorroídos" por las cianobacterias, de origen alóctono. La segunda zona se situaba por debajo de 1 mm de profundidad y estaba formada por capas de acreción con grandes depósitos de carbonato cálcico y cantidades menores de fosfato cálcico de origen biológico. El predominio de un tipo determinado de precipitación mineral que refleja las formas y texturas externas en una zona, p.e., los depósitos de fosfato cálcico similares a una esponja, parece que depende del grupo de microorganismo predominante. **[Int Microbiol** 2006; 9(4):289-295]

Palabras clave: *Microcoleus chthonoplastes* · tapices microbianos · acreción · litificación · biopelículas

Caracterização micromorfológica e litificação das esteiras microbianas do delta do Ebro (Espanya)

Resumo. Estudou-se a organização estrutural, acreção e litificação parcial das esteiras microbianas do delta do Ebro (Espanha), mediante técnicas de microscopia eletrônica de varredura na forma de eléctrons retroespalhados e de microscopia eletrônica de varredura em baixas temperaturas. Uma seção transversal de um fragmento da esteira de 2,5 mm de profundidade, mostrou duas zonas diferenciadas. A primeira é uma camada superior, na qual o microorganismo dominante é *Microcoleus* spp, em crescimento ativo e embebido em uma matriz de exopolissacarideo lassa. Os filamentos de *Microcoleus* estão orientados paralelos à superfície e paralelos entre eles, de modo a se situar de forma perpendicular, mas sem chegar em atravessar-se. A maioria de minerais presentes nesta zona corresponde a grãos de fosfato de cálcio "biocorroidos" pelas cianobacterias, de origem alóctona. A segunda é uma camada abaixo de 1 mm de profundidade, formada por capas de acreção com grandes depósitos de carbonato de cálcio e quantidades menores de fosfato de cálcio de origem biológico. O predomínio de um tipo determinado de precipitação mineral que reflete as formas e texturas externas em uma zona, p.e., os depósitos de fosfato de cálcio similares a esponjas, parecem depender do grupo de microorganismos predominante. [**Int Microbiol** 2006; 9(4): 289-295]

Palavras chave: *Microcoleus chthonoplastes* · esteiras microbianas · acreção · litificação · biofilmes